ARTICLE IN PRESS

Available online at www.sciencedirect.com

ScienceDirect

Quaternary International ▮ (▮▮▮▮) ▮▮▮–▮▮▮

Late Quaternary environmental changes in Misiones, subtropical NE Argentina, deduced from multi-proxy geochemical analyses in a palaeosol-sediment sequence

Michael Zech[a,b,*], Roland Zech[c], Héctor Morrás[d], Lucas Moretti[d], Bruno Glaser[e], Wolfgang Zech[a]

[a]*Chair of Soil Science and Soil Geography, University of Bayreuth, D-95440 Bayreuth, Germany*
[b]*Chair of Geomorphology and Department of Soil Physics, University of Bayreuth, D-95440 Bayreuth, Germany*
[c]*Institute of Geography, University of Bern, 3012 Bern, Switzerland*
[d]*Instituto Nacional de Tecnología Agropecuaria, Castelar, Argentina*
[e]*Department of Soil Physics, University of Bayreuth, D-95440 Bayreuth, Germany*

Abstract

A 4.5-m-long sediment core from a small basin in the Province of Misiones, NE Argentina, was analyzed in a multi-proxy geochemical approach (major and minor elemental composition, C_{org}, N, HI, OI, $\delta^{13}C_{org}$, *n*-alkanes and compound-specific $\delta^{13}C$ analyses of biomarkers) in order to contribute to the reconstruction of the Late Quaternary environmental and climate history of subtropical South America. The results of the elemental analyses and radiocarbon dating indicate different sediment provenances for Unit A—the Holocene, Unit B—the Late Glacial and the Last Glacial Maximum (LGM), and Unit C—the 'Inca Huasi' wet phase (before ~40 ka BP). A sedimentary hiatus after ~40 ka BP is interpreted as a pronounced pre-LGM dry phase with landscape erosion/deflation. Multi-proxy geochemical characterization of the soil organic matter (SOM) shows that especially (i) the stable carbon isotopic composition ($\delta^{13}C$) of the grass-derived alkanes nC_{31} and nC_{33}, (ii) the alkane ratio nC_{31}/nC_{27} and (iii) lacustrine-derived short- and mid-chain alkanes are valuable proxies for the reconstruction of the palaeoenvironment. A transition from C3-tree-dominance to C4-grass-dominance is recorded at the end of the 'Inca Huasi' wet phase. In Unit B, the ratio nC_{31}/nC_{27} documents forest expansion at the beginning of a Late Glacial wet phase. More positive $\delta^{13}C$ values in Unit A reflect the increasing contribution of C4-grasses and/or CAM-plants to the SOM during the Holocene and a human impact on the formation of this unit may be possible. The results are in good agreement with other tropical/subtropical palaeoenvironmental records and highlight the importance and temporal variability of the palaeo-South American Summer Monsoon (SASM).

1. Introduction

Late Quaternary environmental and climate changes in and around tropical and subtropical South America can be reconstructed at high resolution using marine records, lacustrine sediments, speleothems and ice cores (e.g., Salgado-Labouriau, 1997; Behling et al., 2000; Fritz et al., 2004; Cruz et al., 2005; Thompson et al., 2005). Although not at the same temporal resolution, colluvial deposits and palaeosol–loess sequences constitute important terrestrial counterparts (e.g., Teruggi, 1957; Kröhling and Iriondo, 1999; Zárate, 2003; Kemp et al., 2006). In order to derive reliable information about the palaeoenvironmental conditions during sedimentation and to assess post-depositional changes, various geochemical analytical methods are already available and constantly being improved.

During recent decades, the application of stable carbon isotope techniques on organic matter (OM) in palaeosols has contributed significantly to a better understanding of the palaeoenvironment, particularly the reconstruction of the vegetation history. The stable carbon isotopes allow

*Corresponding author at: Chair of Geomorphology and Department of Soil Physics, University of Bayreuth, D-95440 Bayreuth, Germany.
E-mail address: michael_zech@gmx.de (M. Zech).

1040-6182/$ - see front matter © 2008 Elsevier Ltd and INQUA. All rights reserved.
doi:10.1016/j.quaint.2008.06.006

Please cite this article as: Zech, M., et al., Late Quaternary environmental changes in Misiones, subtropical NE Argentina, deduced from multi-proxy geochemical analyses in a palaeosol-sediment sequence. Quaternary International (2008), doi:10.1016/j.quaint.2008.06.006

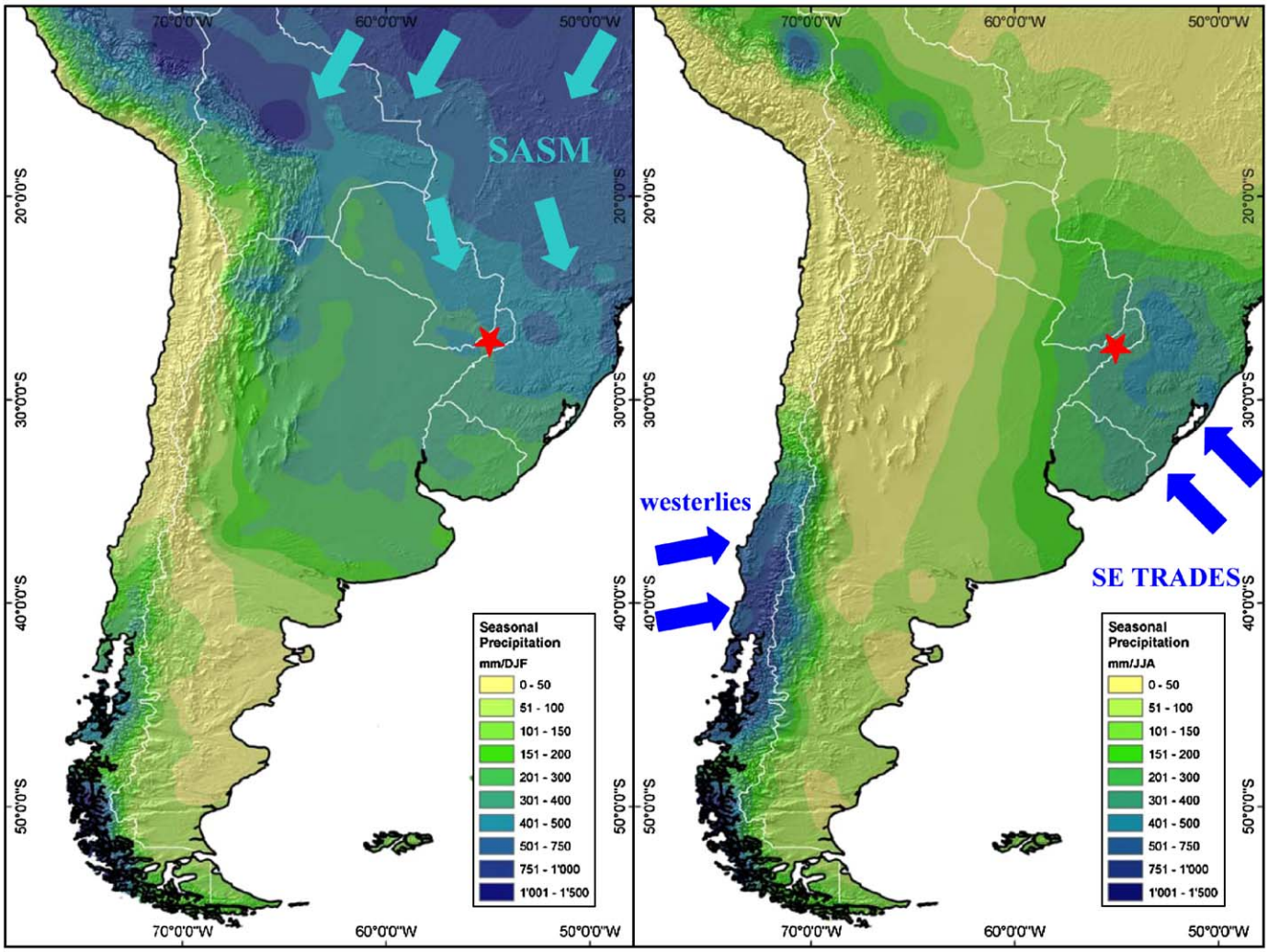

Fig. 1. Location of the Province of Misiones in NE Argentina and seasonal atmospheric circulation patterns providing moisture to the study area (★). Left: rainfall during austral summer (DJF = December January February), SASM = South American Summer Monsoon. Right: rainfall during austral winter (JJA = June July August) (courtesy of May, J.-H.).

differentiating between vegetation types which followed the C3 or the C4 photosynthetic pathway (Aucour et al., 1999; Wang et al., 2000; Freitas et al., 2001; Liu et al., 2005): More positive $\delta^{13}C$ values (approximately −14‰) are characteristic for C4-savannah grasses and more negative $\delta^{13}C$ values (approximately −28‰) are found in trees and C3-grasses. Hence, changes in the carbon isotopic composition in soil or peat profiles or loess–palaeosol sequences can reflect expansion and retreat of forests versus savannah grasslands.

Only since very recently, the combination of gas chromatography with isotope ratio mass spectrometry (GC-C–IRMS) allows the isotopic characterization of individual organic compounds. This potentially reveals more detailed information compared to bulk OM analysis, because (i) during OM degradation a preferential loss of enriched/depleted pools can tamper the original bulk isotope signal and (ii) isotopic information can be obtained from certain compounds that serve as 'biomarkers' (Huang et al., 1996; Lichtfouse, 1998; Street-Perrott et al., 2004; Glaser and Zech, 2005). Such 'biomarkers' ideally originate from certain (groups of) organisms (e.g., higher plants, lacustrine organism, microorganisms, etc.) and hence allow deriving source specific isotope signals.

Apart from the isotopic characterization, also the quantification of biomarkers can be applied in palaeoenvironmental studies. Schwark et al. (2002) and Zech (2006), for instance, used plant-leaf wax-derived long-chain *n*-alkanes (nC_{27}, nC_{29} and nC_{31}) in lacustrine sediments and palaeosols, respectively, to reconstruct vegetation histories.

This study presents results from multi-proxy geochemical analyses that were carried out on palaeosol-sediment samples obtained from a 4.5-m-deep core from Misiones, NE Argentina (Fig. 1). The specific aims are:

- the establishment of a chronostratigraphy, using the major and minor elemental composition combined with radiocarbon dating,

Please cite this article as: Zech, M., et al., Late Quaternary environmental changes in Misiones, subtropical NE Argentina, deduced from multi-proxy geochemical analyses in a palaeosol-sediment sequence. Quaternary International (2008), doi:10.1016/j.quaint.2008.06.006

- the characterization of the soil organic matter (SOM), using standard geochemical parameters like C_{org} content, C_{org}/N ratio, $\delta^{13}C_{org}$ and the hydrogen and oxygen index, respectively (HI and OI),
- the reconstruction of the vegetation history, using $\delta^{13}C$ and *n*-alkanes as biomarkers, and
- the comparison between bulk $\delta^{13}C_{org}$ and compound-specific isotope analyses (CSIA) results obtained for sugars and *n*-alkanes.

Based on these results and in the context of other palaeoenvironmental findings, an attempt is made to draw a conclusive picture of the Late Quaternary environmental and climate changes in Misiones, NW Argentina.

2. Regional setting and modern climate

The Province of Misiones in NE Argentina (25–28°S, 53–56°W, 100–800 m a.s.l.) lies between the Rivers Parana and Uruguay and comprises an area of about 30,000 km^2 (Margalot, 1985) (Fig. 1). Its geological basement is formed by basalts of the Serra Geral Formation which flooded the Paraná Basin during the lower Cretaceous (Zeil, 1986). For more detailed information, the reader is referred to Morrás et al. (2008) and references therein. Geomorphologically, Misiones is a peneplain and it can be divided into nine regions (Ligier et al., 1990). The central plateau constitutes the water divide between the Rio Paraná and the Rio Uruguay and increases from 300 m in the south to about 600 m a.s.l. in the central part. The undulated relief reveals slopes with inclinations of up to 9%. According to Iriondo and Kröhling (2004), loess of Late Pleistocene–Holocene age (the so-called Oberá Formation) mantles the Province of Misiones and neighboring areas of Brazil and Paraguay with a typical thickness between 3 and 8 m. In contrast, Morrás et al. (2005) suggested that in situ weathering rather than eolian transport is the source for the soil parent material. The existence of this 'tropical loess' is still discussed controversially (Iriondo and Kröhling, 2004; Morrás et al., 2008).

The original vegetation cover in Misiones mainly consisted of mesophytic subtropical forests with large proportions of evergreen species (Hueck and Seibert, 1972). Current land use converted large areas into commercial plantations with non-native *Pinus* (190,000 ha) and *Eucalyptus* (15,000 ha). The native timber tree, *Araucaria angustifolia* (*Bert*) *O. ktze* covers 20,000 ha (Fernández and Lupi, 1999).

The South American climate is characterized by three dominant circulation regimes (Fig. 1): (i) the westerlies, which provide Pacific moisture to the southwest (Patagonia); (ii) the SE trades, which advect moisture to regions near the Atlantic coast (NE Argentina, Uruguay and SE Brazil); and (iii) the South American Summer Monsoon (SASM) and the South Atlantic Convergence Zone (SACZ), respectively, which result in an austral summer precipitation maximum in tropical/subtropical South America (Cerveny, 1998; Zhou and Lau, 1998; Vera et al., 2002; Gan et al., 2004). Misiones receives the highest rainfalls of Argentina except for the southern cordillera (mean annual precipitation ~1700 mm). This is due to the combined influence of high summer and winter precipitation as illustrated in Fig. 1 and manifests in a double rainy season (Prohaska, 1976).

3. Materials and methods

In September 2004, a 4.5-m-long sediment core ('Arg. D4') was taken with a piston corer from a weakly flooded small basin located northeast of the city Oberá (27°23′35″S, 55°31′52″W; 330 m a.s.l.; see Fig. 1). For a more detailed map, see Fig. 2 of Morrás et al. (2008), who also provide detailed sedimentological and micromorphological results for the study area. The basin has a diameter of about 800 m and its seasonally swampy central part nowadays is only drained after high precipitation. Before sub-sampling, the core at 5 cm intervals for geochemical analysis, color, grain size and soil morphological features were documented in the field (see also Fig. 2a): The upper 60 cm were characterized by black, intensively rooted, silty fine sand. Below, an abrupt change to very dense, light gray, mottled clay could be observed. At about 1.4 m depth, the compact sediments became darker again with embedded gray, mottles between 1.7 and 2.5 m depth. A light gray silty layer from 2.5 to 2.9 m depth with an intercalated thin humus band separated these deposits from underlying dark sediments, which continued down to 3.2 m depth. From 3.2 to 3.6 m depth, the mottled and now coarser grained material became paler again. Below are very dense light gray sediments with hydromorphic features (from 3.6 to 4.0 m depth) covering the reddish brown and probably saprolytic parent material at >4.0 m depth.

Geochemical analyses were done on air-dried, homogenized sample aliquots. Small amounts of carbonate (<1%) were present from 30 to 100 cm depth and in the light gray band between 2.5 and 2.9 m depth. *Major and minor elemental compositions* were determined using a Philips 2404 X-ray fluorescence spectrometer. The weathering indices A and B were calculated according to Kronberg and Nesbitt (1981) following the equations:

$$\text{weathering index A} = \frac{SiO_2 + Na_2O + K_2O + CaO}{Al_2O_3 + SiO_2 + Na_2O + K_2O + CaO},$$

$$\text{weathering index B} = \frac{Na_2O + K_2O + CaO}{Al_2O_3 + Na_2O + K_2O + CaO}.$$

Total organic carbon (C_{org}) *and total nitrogen* (N) were measured using dry combustion of a finely ground, homogeneous and decalcified 50 mg sub-sample followed by thermal conductivity detection on a Vario EL elemental analyzer (Elementar, Hanau, Germany). The detection limits of the machine were calculated by measuring blanks with increasing net weights of wolfram oxide in tin capsules (~0.0002% for C and ~0.007% for N).

Please cite this article as: Zech, M., et al., Late Quaternary environmental changes in Misiones, subtropical NE Argentina, deduced from multi-proxy geochemical analyses in a palaeosol-sediment sequence. Quaternary International (2008), doi:10.1016/j.quaint.2008.06.006

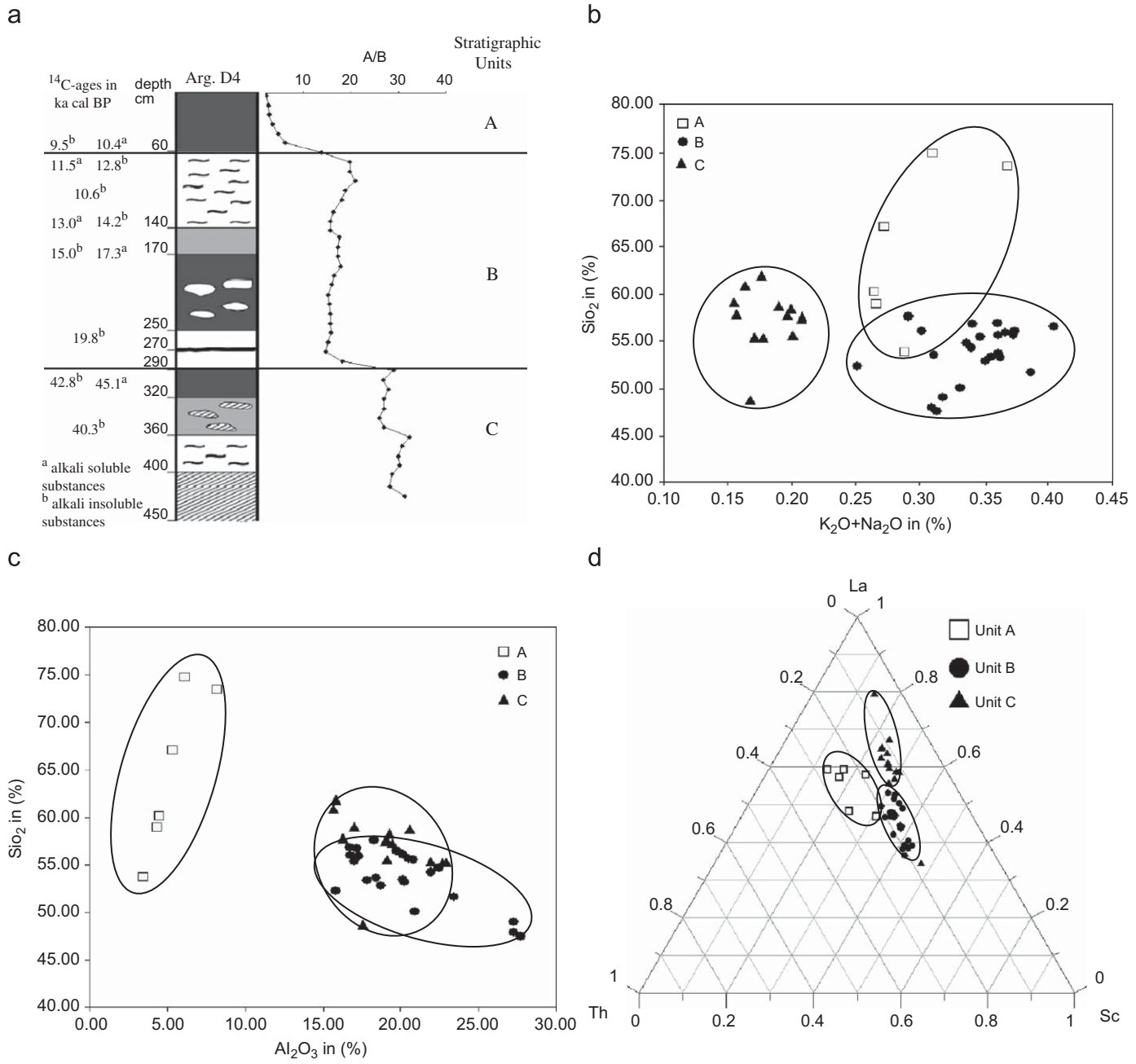

Fig. 2. (a) Schematic stratigraphy and numeric dating results for the sediment core Arg. D4, depth function for the ratio of the weathering indices A and B, and subdivision of the core into the stratigraphic Units A, B and C. (b) Cross-plot diagrams for SiO_2 versus $Na_2O + K_2O$, and (c) SiO_2 versus Al_2O_3. (d) Ternary diagram for the immobile trace elements Sc, Th and La.

Further information about the elemental composition of the OM was obtained by Rock-Eval pyrolysis (→*Hydrogen and Oxygen Index, HI and OI*). The analytical procedure comprises progressive heating of sediment samples and measurements of the amounts of hydrocarbons that escape at different temperatures. This method was initially developed to measure both the free hydrocarbon content and the hydrocarbons released by thermal conversion of kerogen in rock and sediment samples (Espitalie et al., 1985). The HI estimates the amount of hydrogen contained in the sedimentary OM (expressed as mg hydrocarbons $g^{-1} C_{org}$), whereas the OI represents the amount of oxygen in mg $CO_2\, g^{-1} C_{org}$. These parameters hence roughly correspond to the H/C and O/C ratios of OM.

Several authors have used the Rock-Eval pyrolysis to characterize lake sediments and interpreted the HI and OI in terms of origin of the OM and/or degree of OM oxidation (Ariztegui et al., 2001; Lüniger and Schwark, 2002; Filippi and Talbot, 2005). Recently, Disnar et al. (2003) applied this technique to a variety of soil profiles and found the parameters HI and OI to be diagnostic for SOM alteration.

Please cite this article as: Zech, M., et al., Late Quaternary environmental changes in Misiones, subtropical NE Argentina, deduced from multi-proxy geochemical analyses in a palaeosol-sediment sequence. Quaternary International (2008), doi:10.1016/j.quaint.2008.06.006

The $\delta^{13}C$ values of the bulk OM ($\delta^{13}C_{org}$) were measured using dry combustion of a 40 mg decalcified sub-sample with a Carlo Erba NC 2500 elemental analyzer coupled to a Delta^{plus} continuous flow IRMS via a Conflow II interface (Thermo Finnigan MAT, Bremen, Germany). Sucrose (CH-6, IAEA, Vienna, Austria) and $CaCO_3$ (NBS 19, Gaithersburg, USA) were used as calibration standards. Natural abundances of stable carbon isotopes are expressed in the usual δ-scale in parts per thousand according to the equation:

$$\delta_{sample}\,(‰) = \left(\frac{R_{sample} - R_{standard}}{R_{standard}}\right) \times 1000,$$

where R_{sample} and $R_{standard}$ are the $^{13}C/^{12}C$ abundance ratios of a sample or a standard, respectively. Precision was determined by measuring known standards in replication (~0.15‰ for $\delta^{13}C$ and 0.25‰ for $\delta^{15}N$).

$\delta^{13}C_{org}$ allows the reconstruction of the vegetation history in cases where the latter coincided with a C3/C4 change. As the C4 metabolic pathway is especially competitive under drier conditions (Collatz et al., 1998), palaeoclimatic implications can be drawn. However, pedogenetic processes (e.g., SOM degradation, methanogenesis) do not only affect degradation proxies like the C_{org}/N ratio, HI and OI, but can potentially also tamper the $\delta^{13}C_{org}$ signal, for example, by selective removal of isotopically enriched/depleted pools. This may weaken the validity of the bulk $\delta^{13}C_{org}$ signal for the reconstruction of the vegetation history.

Contrariwise, it is assumed that such isotopic adulteration is more negligible on molecular level (Cranwell, 1981; Street-Perrott et al., 1997). Therefore, biomarkers were tested for their applicability to confirm the bulk $\delta^{13}C_{org}$ results. Street-Perrott et al. (2004), for instance, used CSIA in lacustrine OM to trace Late Quaternary changes in the terrestrial and aquatic carbon cycle by determining the $\delta^{13}C$ values of source-specific compounds like *n*-alkanes and lignin phenols. Concerning the plant-leaf wax-derived *n*-alkanes, Collister et al. (1994) showed that they reveal characteristically different $\delta^{13}C$ values depending on the metabolic pathway (C3 or C4) and several studies considered them to be more diagnostic than bulk OM when assessing the input contribution of C3 versus C4 plants (Huang et al., 2001; Feng, 2002; Street-Perrott et al., 2004).

Glaser and Zech (2005) additionally investigated the isotopic composition of neutral sugars, such as the plant-derived pentoses arabinose and xylose and the microbial-derived deoxyhexoses fucose and rhamnose, to characterize lacustrine sediments and to reconstruct climate and landscape changes.

For the extraction of *n*-alkanes, an accelerated solvent extractor (Dionex ASE 200) was used. Free lipids were extracted with methanol/toluene (7/3) at 9×10^6 Pa and a temperature of 120 °C, followed by *n*-alkane separation on columns with activated (5%) aluminum oxide (2 g) above activated (5%) silica (2 g) and 45 ml hexane/toluene (85/15) as elution solvent (Bourbonniere et al., 1997). For quantification, an HP 6890 GC equipped with a flame ionization detector (FID) and deuterated *n*-alkanes (d_{42}-*n*-C_{20} and d_{50}-*n*-C_{24}) as internal standards were used.

Long-chain *n*-alkanes (nC_{25}–nC_{33}) with a pronounced odd-over-even predominance of carbon atoms are incorporated in cuticular plant-leaf waxes (Kolattukudy, 1976; Collister et al., 1994). As they are assumed to be relatively resistant to degradation (Cranwell, 1981; Meyers and Ishiwatari, 1993), they are used as biomarkers in palaeoenvironmental studies (e.g., Bourbonniere et al., 1997; Ficken et al., 1998; Glaser and Zech, 2005). Apart from the isotopic characterization of the alkanes, the *n*-alkane pattern in the palaeosol-sediment record was used in order to distinguish between OM derived from grasses versus OM derived from trees. Several studies have shown that nC_{31} dominates in most grasses/herbs, whereas nC_{27} dominates in most trees/shrubs and used this difference for the reconstruction of the palaeovegetation (Cranwell, 1973; Nott et al., 2000; Schwark et al., 2002). Furthermore, it is well known that the short-chain alkanes nC_{17}, nC_{18} and nC_{19} in lake sediments are mainly from algal origin (Meyers and Ishiwatari, 1993; Bourbonniere et al., 1997) and recently Ficken et al. (2000) and Zhang et al. (2004) reported that the mid-chain alkanes nC_{23} and nC_{25} in lake sediments originate mainly from submerged plants.

Plant- and microbial-derived sugars were determined—after addition of 100 μg myo-inositol as the first internal standard—on selected samples (containing 7–8 mg TOC). Hydrolysis with 10 mL 4 M trifluoroacetic acid (4 h, 105 °C) and purification were carried out according to Amelung et al. (1996). After hydrolysis, samples were filtered, dried using a rotary evaporator and re-dissolved in approximately 10 mL distilled water. For sample purification, an adsorption resin (XAD-7) and a cation exchange resin (Dowex 50 W X8) were used. Eluates from these resins containing the sugars were freeze-dried prior to derivatization using the methylboronic acid (MBA) derivatization technique (Gross and Glaser, 2004). Prior to derivatization of the samples, 100 μg of 3-*O*-methylglucose in pyridine was added as recovery standard, 4.5 mg of MBA in pyridine was added to the freeze-dried sugar extracts and the mixture heated to 60 °C for 60 min. Then, 50 μL BSTFA was added and the mixture heated at 60 °C for exactly 5 min.

The *compound-specific* $\delta^{13}C$ *values* of the individual *n*-alkane and sugar molecules were determined by GC-C–IRMS using a Trace GC 2000 equipped with a split–splitless injector coupled via a Combustion III interface to a Delta^{plus} continuous flow IRMS (all Thermo Finnigan MAT, Bremen, Germany). To correct for any isotopic fractionation caused by derivatization and measurement, especially during vaporization in the injector port (Schmitt et al., 2003), a suite of six standards with increasing analyt amounts was derivatized and analyzed accordingly. Each sample batch comprising a maximum of 20 samples was analyzed at least in triplicate. From the standards,

Please cite this article as: Zech, M., et al., Late Quaternary environmental changes in Misiones, subtropical NE Argentina, deduced from multi-proxy geochemical analyses in a palaeosol-sediment sequence. Quaternary International (2008), doi:10.1016/j.quaint.2008.06.006

Table 1
Radiocarbon dates (KIA: Leibniz Laboratory, University of Kiel, Germany; Poz: Poznan Radiocarbon Laboratory, Poland; Erl: Physics Department of the University of Erlangen, Germany)

Sample	Lab. number	Depth (cm)	Material	Uncalibrated ^{14}C (a BP)	Calibrated ^{14}C (a cal BP)	Chronostratigraphic interpretation
Arg.04/D4/6B	KIA30161	57.5	HA[a]	9255±40	10422±78	Early Holocene
Arg.04/D4/6B	KIA30161	57.5	H[b]	8470±45	9495±26	Early Holocene
Arg.04/D4/8A	KIA26094	72.5	HA	10025±60	11548±169	Late Glacial
Arg.04/D4/8A	KIA26094	72.5	H	10890±50	12847±81	Late Glacial
Arg.04/D4/10A	KIA26095	92.5	H	9384±45	10620±53	Late Glacial
Arg.04/D4/14	KIA26096	135.0	HA	11069±193	13006±187	Late Glacial
Arg.04/D4/14	KIA26096	135.0	H	12149±50	14190±237	Late Glacial
Arg.04/D4/18A	KIA26097	172.5	H	12654±55	15022±294	Late Glacial
Arg.04/D4/18A	KIA26097	172.5	HA	13908±105	17302±125	LGM/Late Glacial
Arg.04/D4/26B	Poz-12818	257.5	H	16490±90	19809±292	LGM
Arg.04/D4/31B	Poz-12925	307.5	H	37900±900	42817±609	MIS 3
Arg.04/D4/31B	Poz-15662	307.5	HA	41400±1300	45134±1271	MIS 3
Arg.04/D4/36B	Poz-12926	357.5	H	34500±600	40332±853	MIS 3
Arg.03/P2	Erl-6147	240.0	H	14368±102	17700±235	LGM/Late Glacial
Arg.03/D2	Erl-6148	140.0	H	30460±284	35682±307	MIS 3

Calibration was outlined with quickcal2005 version 1.4 (http://www.calpal-online.de).
[a]HA: alkali soluble substances (humic acids).
[b]H: alkali insoluble substances (humines).

corrections for the amount-dependent isotope fractionation during GC-C–IRMS measurements were calculated as outlined by Glaser and Amelung (2002). Further details will be given in Zech and Glaser (2008).

Fifteen AMS radiocarbon ages were obtained for acid and/or alkali insoluble fractions extracted from eight samples of the core Arg. D4 and two samples deriving from other sediment cores taken in the study area (Arg. 03/P2 and Arg. 03/D2). All radiocarbon ages were corrected for the $^{13}C/^{12}C$ ratio and additionally calibrated with quickcal2005 version 1.4 (http://www.calpal-online.de). Both uncalibrated and calibrated ages are given in Table 1. For reasons of simplicity, reference is made only to calibrated ages in the text and in Figs. 2 and 3.

4. Results

This section presents the results of the X-ray fluorescence analyses and the radiocarbon ages aiming at the establishment of a chronostratigraphy for the palaeosol-sediment record. The SOM is characterized based on the parameters C_{org}, C_{org}/N, $\delta^{13}C_{org}$, HI and OI. Subsequently, the *n*-alkane biomarker data are presented and used to reconstruct the vegetation history and, finally, the results from the compound-specific $\delta^{13}C$ analyses are discussed.

4.1. Chronostratigraphy

The depth functions of most major and minor elements show distinct shifts at 60 and 290 cm depth, respectively. This is illustrated exemplarily in Fig. 2a, where the ratio of the weathering indices A and B (according to Kronberg and Nesbitt, 1981) is plotted versus depth. These results suggest that the sedimentary material is not homogeneous but stratified. This can be corroborated by plotting SiO_2 versus Na_2O+K_2O (Fig. 2b) and SiO_2 versus Al_2O_3 (Fig. 2c). Such cross-plot diagrams are frequently used to evaluate the transformation of feldspars to clay minerals (Garrels and Mackenzie, 1971; McLennan, 1993) and to depict compositional variability of silty material (Gallet et al., 1998; Muhs et al., 2004). Similar diagrams can be plotted for immobile trace elements, which also allow identification of different sources of sediments (Muhs et al., this issue). In Fig. 2d, for example, a ternary diagram for the elements Sc, Th and La is shown. All these diagrams depict well-discernable clusters for the samples from 0 to 60, 60 to 290 and 290 to 425 cm depth. These findings suggest distinguishing at least three stratigraphic units (A, B and C; see Fig. 2), which indicates that the core comprises several periods of sedimentation.

Erosive discordances in eolian sediments in northern Argentina have previously been described and seem to be common features (Zárate, 2003; Iriondo and Kröhling, 2004; Kemp et al., 2006). Therefore, the abrupt shifts in the elemental composition are interpreted as erosive events—possibly by means of deflation—which may have truncated the palaeosol-sediment sequence under study before sedimentation proceeded.

To provide a chronological framework for the palaeoenvironmental events recorded in the sediment core, eight soil samples were dated by radiocarbon analyses. The ^{14}C-ages obtained for alkali soluble and/or alkali insoluble substances are illustrated in Figs. 2 and 3 and listed in Table 1. Two samples from the lowermost Unit C yielded calibrated ages between 40.3 and 45.1 ka cal BP, five samples from Unit B gave ^{14}C-ages between 10.6 and 19.8 ka cal BP.

Please cite this article as: Zech, M., et al., Late Quaternary environmental changes in Misiones, subtropical NE Argentina, deduced from multi-proxy geochemical analyses in a palaeosol-sediment sequence. Quaternary International (2008), doi:10.1016/j.quaint.2008.06.006

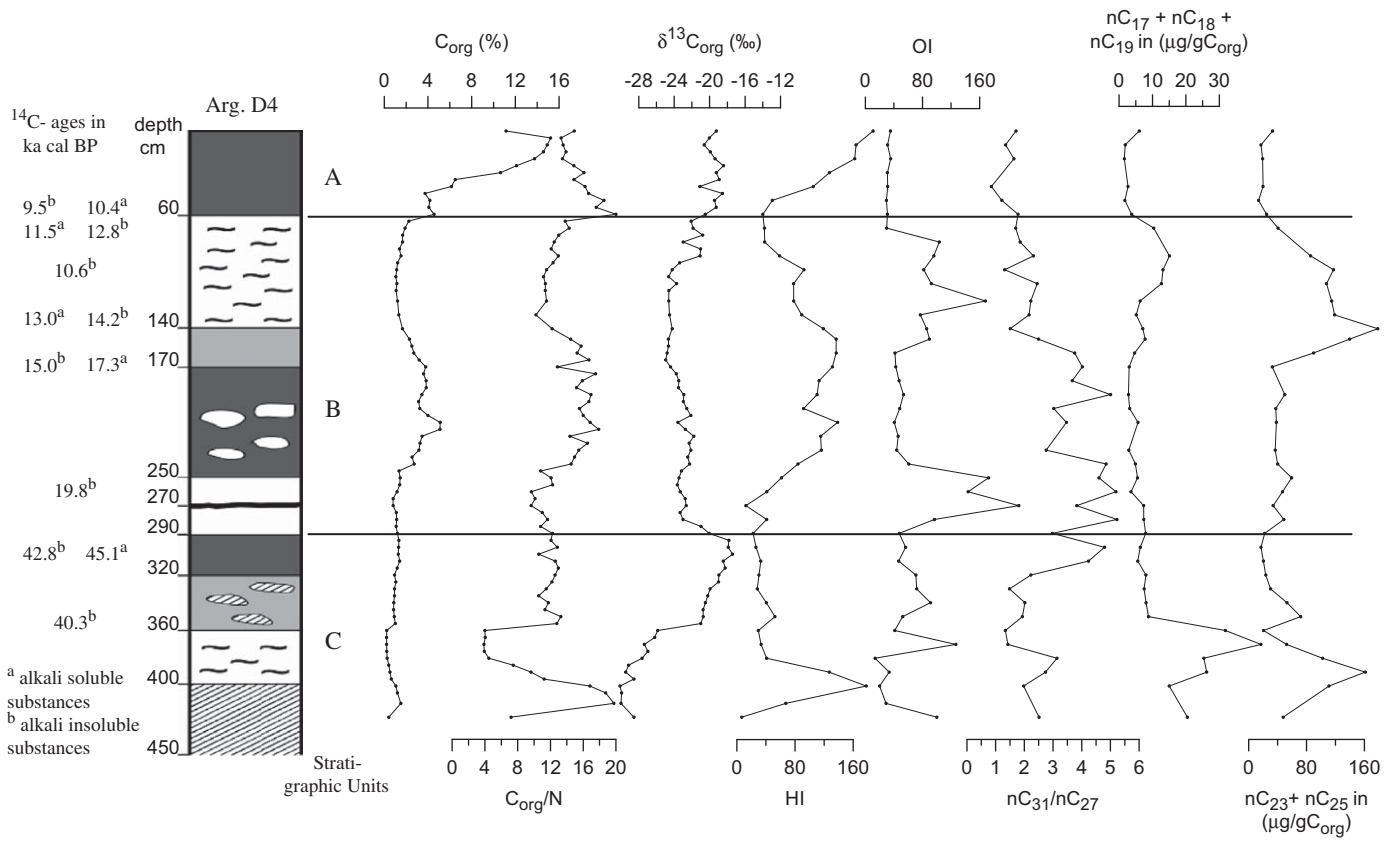

Fig. 3. Left: schematic stratigraphy and numeric dating results for the sediment core Arg. D4, and stratigraphic subdivision. Right: depth functions for C_{org}, C_{org}/N, $\delta^{13}C_{org}$, HI, OI and the biomarker proxies nC_{31}/nC_{27}, $nC_{17}+nC_{18}+nC_{19}$ and $nC_{23}+nC_{25}$.

Humic acids at the bottom of Unit A were 10.4 ka old, whereas alkali insoluble substances from the same sample yielded an age of 9.5 ka cal BP. Considering the uncertainties of radiocarbon dating in sediments (Geyh and Schleicher, 1991), all ages are more or less consistent despite of two minor age inversions (10.6 and 40.3 ka cal BP).

Overall, the numeric dating results (i) confirm the distinction of at least three stratigraphic units and (ii) allow the establishment of a tentative chronostratigraphy: the sediments of Unit C were deposited at/before ~40 ka BP, i.e., likely during Marine Isotope Stage (MIS) 3 or earlier, Unit B represents the Last Glacial Maximum (LGM) and the Late Glacial, and Unit A started to developed during the Early Holocene.

4.2. Characterization of the organic matter

The depth functions of C_{org}, C_{org}/N, $\delta^{13}C_{org}$, HI, OI and the alkane ratio nC_{31}/nC_{27} are shown in Fig. 3. C_{org} decreases sharply below 30 cm depth in Unit A. High C_{org} values around 15% in the upper decimeters indicate considerable recent biomass production. In Units B and C, the values range from 0.21% to 5.1% with C_{org} being higher than 2% from 1.5 to 2.5 m depth. Distinct C_{org} minima around 1.0 and 3.8 m depth coincide with sediments characterized by hydromorphic features. These horizons also depict low C_{org}/N ratios, which vary in concert with C_{org} in Unit C ($R = 0.87$, $n = 26$) and Unit B ($R = 0.85$, $n = 43$). On the contrary, C_{org} and C_{org}/N correlate negatively in Unit A ($R = -0.89$, $n = 12$).

Apart from the observation that the transition from Unit A to B reveals a distinct shift in the C_{org}/N ratios and therefore confirms the stratigraphy, a more detailed and straightforward interpretation of C_{org} and C_{org}/N concerning the palaeoenvironmental conditions is challenging, because both proxies are subject to various factors influencing them. The C_{org} content mainly depends both on primary production and on SOM mineralization. Also low C_{org}/N ratios may on the one hand indicate intensive SOM mineralization and hence the release of CO_2. On the other hand, lacustrine phytoplankton is characterized by low C_{org}/N ratios (e.g., Silliman et al., 1996) and could have become an important source for OM when a shallow lake possibly developed under more humid conditions (at around 1 m depth and from 3.6 to 4.0 m depth).

Further palaeoenvironmental information can be derived from the stable carbon isotopic composition of the OM ($\delta^{13}C_{org}$). It varies between −30‰ and −18‰ (Fig. 3). Unit C shows a general upward trend from the most negative to the most positive values in the palaeosol-sediment sequence and a sudden shift of almost 5‰ at 3.6 m depth. The lower meter of Unit B has $\delta^{13}C$ values around −23‰. From 1.7 to 1.0 m depth, the values are

Please cite this article as: Zech, M., et al., Late Quaternary environmental changes in Misiones, subtropical NE Argentina, deduced from multi-proxy geochemical analyses in a palaeosol-sediment sequence. Quaternary International (2008), doi:10.1016/j.quaint.2008.06.006

~−25‰ and the upper decimeters of Unit B reveal the transition to again more positive values as observed in Unit A (~−20‰).

Principally, smaller $\delta^{13}C$ variations in plants and sediments can be caused by both environmental factors like water stress or changes in the atmospheric CO_2 (concentration and isotopic signature) and by pedogenetic processes like SOM degradation or methanogenesis (discussed in details, e.g., in Zech et al., 2007). However, the pronounced trends of several per mille in the record can only be interpreted in terms of photosynthetic pathway changes of the surrounding vegetation, which also allow palaeoclimatic implications as it is well known that the C4-grasses are especially competitive under relatively drier/warmer conditions (Collatz et al., 1998). Accordingly, $\delta^{13}C$ in Unit C (Fig. 3) documents that C3 vegetation first dominated during MIS 3 and was then replaced increasingly by C4-savannah grasses or succulent plants using the *Crassulacean* acid metabolism (CAM). The $\delta^{13}C_{org}$ results for Units A and B indicate that changes of the photosynthetic pathway (C3/C4/CAM) also occurred in the study area since the LGM. Whereas the C3 photosynthetic pathway dominated from 1.0 to 2.9 m depth, C4-savannah grasses and/or CAM-plants started to expand since the Holocene. For reasons of simplicity, the subsequent discussions neglect the CAM-plants and are restricted to the C3 and C4 photosynthetic pathway.

Fig. 3 illustrates the HI and OI depth functions in the core, showing distinct variations: The HI values range from 7 to 187 and are especially increased in the uppermost decimeters of Unit A, from 1.5 to 2.5 m depth in Unit B and in the lowermost decimeters of Unit C. They correlate with TOC ($R = 0.64$, $n = 43$) and C/N ($R = 0.42$, $n = 43$) indicating that OM in these TOC enriched horizons is less degraded than the more dehydrogenated OM at approximately 0.7 m depth and in the upper part of Unit C. In the course of humus degradation, the dehydrogenation (HI decreases) is progressively followed by a gain in oxygen (OI increase). OI values obtained for Arg. D4 range from 14 to 215 with OI maxima occurring both in the uppermost and lowermost decimeters of Unit B (Fig. 3). This could indicate that the SOM between 0.6 and 1.5 m and between 2.5 and 2.9 m depth is intensively degraded. However, small amounts of carbonate (<1%) were detected both in the light gray horizon from 2.5 to 2.9 m depth and from 0.3 to 1.0 m depth. Therefore, an inorganic contamination of the OI signal has to be accounted for.

4.3. Lacustrine biomarkers

The concentrations of short-chain alkanes are generally low in the record (<10 μg $\sum(nC_{17}$–$nC_{19})$ g C_{org}^{-1}). However, distinctly increased values (>15 μg) in the uppermost decimeters of Unit B and in the lower part of Unit C coincide with low C_{org}/N ratios (Fig. 3). As it is well known that the alkane pattern of many algae are dominated by short-chain homologs (Meyers and Ishiwatari, 1993; Bourbonniere et al., 1997), these results point to lacustrine conditions presumably having prevailed during the deposition of these sediments. This interpretation is furthermore corroborated by mid-chain alkane maxima ($\sum(nC_{23}$, $nC_{25})$) occurring in these horizons (Fig. 3). Recently, these homologs were found to dominate the alkane pattern of submerged plants in lakes and were consequently used in a proxy ratio (P_{aq}) to reconstruct lake histories (Ficken et al., 2000; Zhang et al., 2004). Although these findings are important for the palaeoenvironmental and palaeoclimatic interpretation of Arg. D4, SOM in the record nevertheless predominantly originates from terrestrial plants.

4.4. *n*-Alkane ratio C_{31}/C_{27} as proxy for the palaeovegetation

Typical GC-FID chromatograms for *n*-alkanes extracted from higher plant samples in Misiones are shown in Fig. 4. They reveal the tree- and shrub-characteristic predominance of nC_{27} and nC_{29} for (A) *Prosopis* sp. and the grass- and herb-characteristic predominance of the alkane nC_{31} for (B) *Setaria* sp. A ternary diagram with the alkanes nC_{27}, nC_{29} and nC_{31} therefore depicts a typical cluster for most grass samples close to nC_{31}, whereas most trees/shrubs cluster close to nC_{27} (Fig. 5). The results are hence in agreement with findings from other authors using these two *n*-alkanes for the reconstruction of palaeovegetation (Cranwell, 1973; Farrimond and Flanagan, 1996; Schwark et al., 2002).

Fig. 3 illustrates the depth function for the alkane ratio nC_{31}/nC_{27} obtained for the core Arg. D4. The ratio ranges from 0.9 to 5.2 and serves as a proxy for grasses and herbs versus trees and shrubs. The increase of C4-savannah grasses in Unit C, which was already deduced from the $\delta^{13}C_{org}$, is corroborated by the biomarker results showing a trend to a wider ratio of nC_{31}/nC_{27}. The opposite trend from Unit B to A reflects the re-expansion of forests since the LGM. Although according to the biomarker results, trees and shrubs already contributed to the SOM around 18 ka cal BP, a marked forest retreat is indicated by the alkane ratio from 2.0 to 1.6 m depth. Ratios from 0.9 to 2.4 above 1.5 m depth document a mixed tree/grass vegetation cover since the Late Glacial and suggest that grasses did not re-expanded significantly since then. The increasing $\delta^{13}C_{org}$ values in Unit A would therefore have to be interpreted as suppression of C3-grasses by C4-grasses in the tree–grass-landscape rather than as increasing dominance of grasslands over forests.

4.5. Compound-specific $\delta^{13}C$ values of the biomarkers

Pedogenetic processes may tamper bulk SOM $\delta^{13}C$ values. Here, the applicability of isotope analyses on individual compounds for palaeoenvironmental reconstructions is tested. Results for the sugars are illustrated in Fig. 6a, those for *n*-alkanes in Fig. 6b. Except for rhamnose, the sugars are a generally enriched pool with

Please cite this article as: Zech, M., et al., Late Quaternary environmental changes in Misiones, subtropical NE Argentina, deduced from multi-proxy geochemical analyses in a palaeosol-sediment sequence. Quaternary International (2008), doi:10.1016/j.quaint.2008.06.006

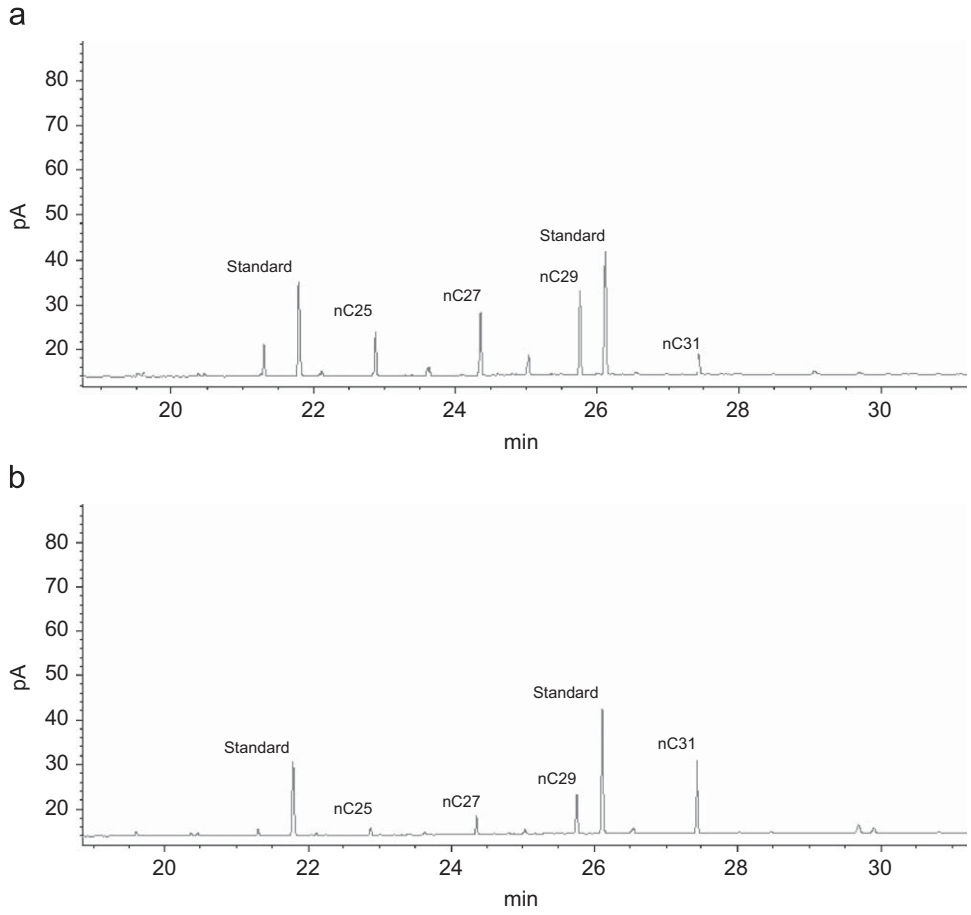

Fig. 4. GC-FID chromatograms for (a) the shrub sample *Prosopis* sp. and (b) the grass sample *Setaria* sp.

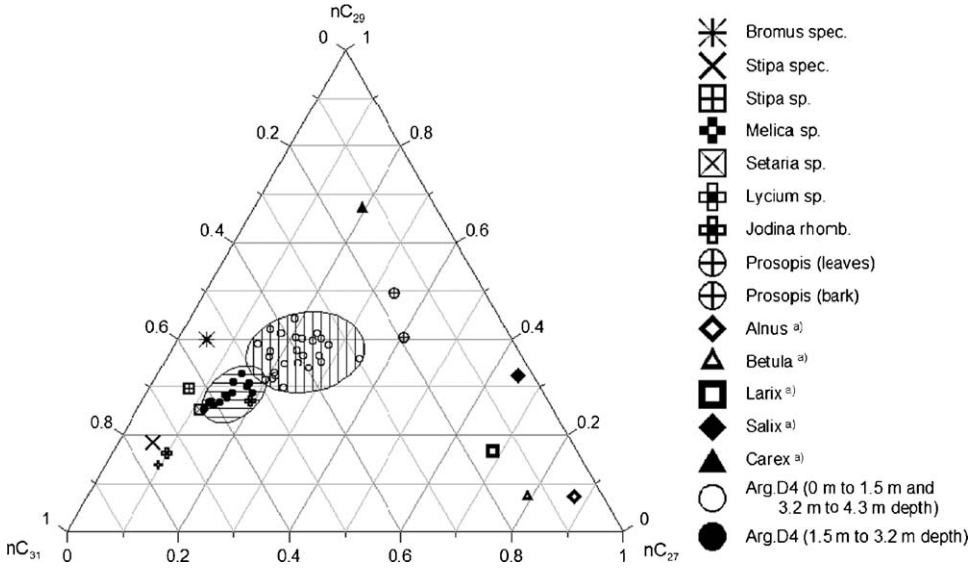

Fig. 5. Ternary diagram with the *n*-alkanes C_{27}, C_{29} and C_{31} for plant samples and Arg. D4 sediment samples (in shaded clusters). Whereas grasses cluster close to nC_{27}, trees and shrubs cluster closer to nC_{29} and nC_{31}. (a) Own data from another study site.

more positive $\delta^{13}C$ values (ranging from about −31‰ to −11‰) in comparison to bulk SOM. On the contrary, the long-chain *n*-alkanes nC_{27}, nC_{29}, nC_{31} and nC_{33} are clearly depleted in the heavier ^{13}C (ranging from about −40‰ to −19‰). This is in agreement with findings from other authors (van Dongen et al., 2002; Glaser, 2005).

In Unit C, the $\delta^{13}C$ values of the individual sugars correlate with bulk $\delta^{13}C_{org}$ ($R > 0.75$, $n = 6$). In Units A

Please cite this article as: Zech, M., et al., Late Quaternary environmental changes in Misiones, subtropical NE Argentina, deduced from multi-proxy geochemical analyses in a palaeosol-sediment sequence. Quaternary International (2008), doi:10.1016/j.quaint.2008.06.006

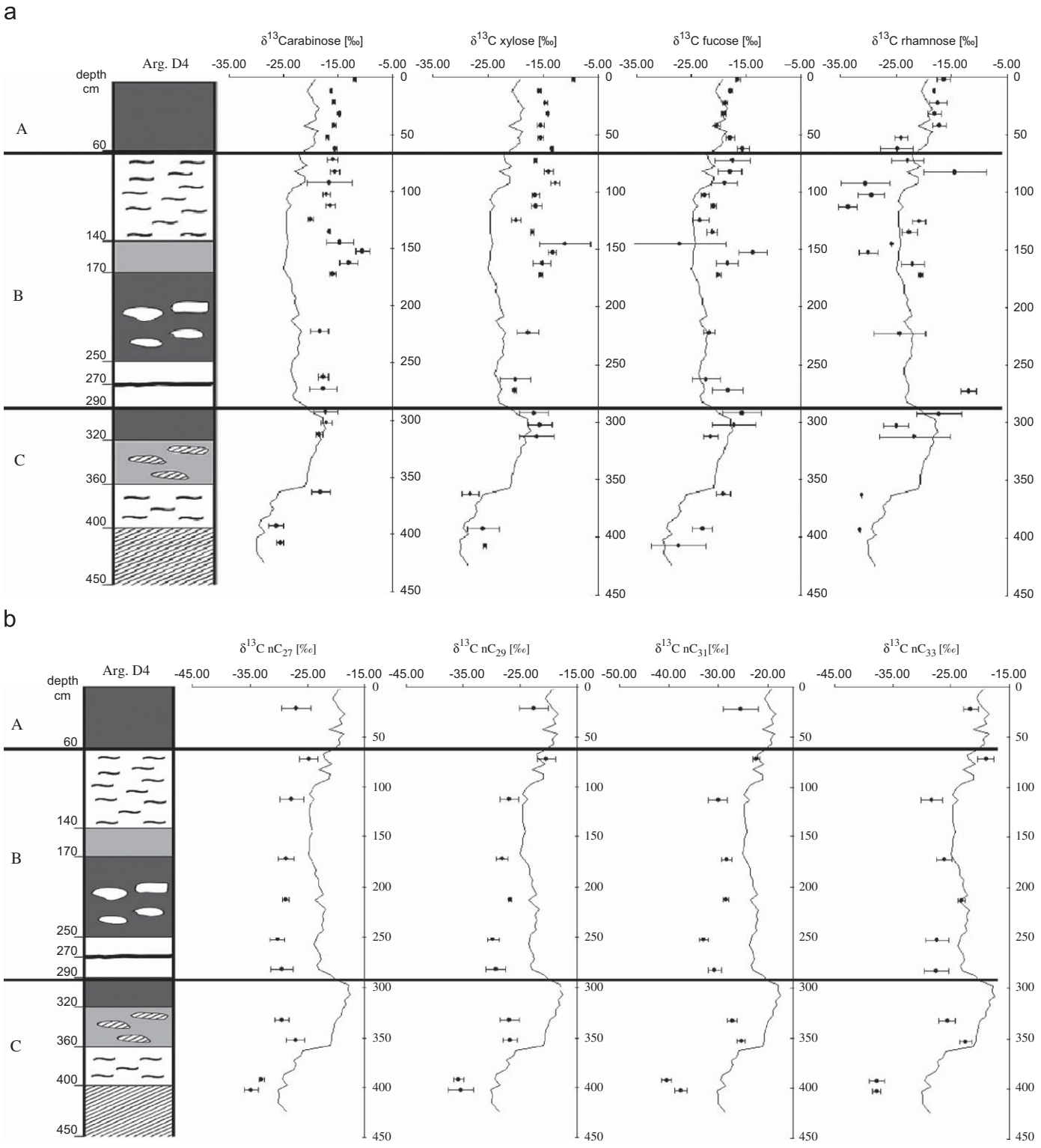

Fig. 6. (a) Compound-specific $\delta^{13}C$ values of plant- (arabinose and xylose) and microbial-derived sugar monomers (fucose and rhamnose). (b) Compound-specific $\delta^{13}C$ values of individual plant-leaf wax-derived *n*-alkanes. Modified after Zech and Glaser (2008).

and B ($n = 21$), this correlations seems to hold only for the microbial-derived sugars fucose and rhamnose ($R > 0.50$), but not for the plant-derived sugars arabinose and xylose ($R < 0.11$). The microbial detritus mainly reflects the isotopic signature of microbial food, i.e., the $\delta^{13}C_{org}$ variations of the SOM. The discrepancy between the $\delta^{13}C$ values of the plant-derived sugars and bulk $\delta^{13}C_{org}$ in the Units A and B may be explained with either (i) bulk $\delta^{13}C_{org}$ being tampered by pedogenetic processes like mineralization ($\rightarrow \delta^{13}C_{org}$ would hence not be interpretable in terms of an C3/C4 input signal), or (ii) with arabinose and xylose not being suitable biomarkers for the (bulk-)plant-derived

Please cite this article as: Zech, M., et al., Late Quaternary environmental changes in Misiones, subtropical NE Argentina, deduced from multi-proxy geochemical analyses in a palaeosol-sediment sequence. Quaternary International (2008), doi:10.1016/j.quaint.2008.06.006

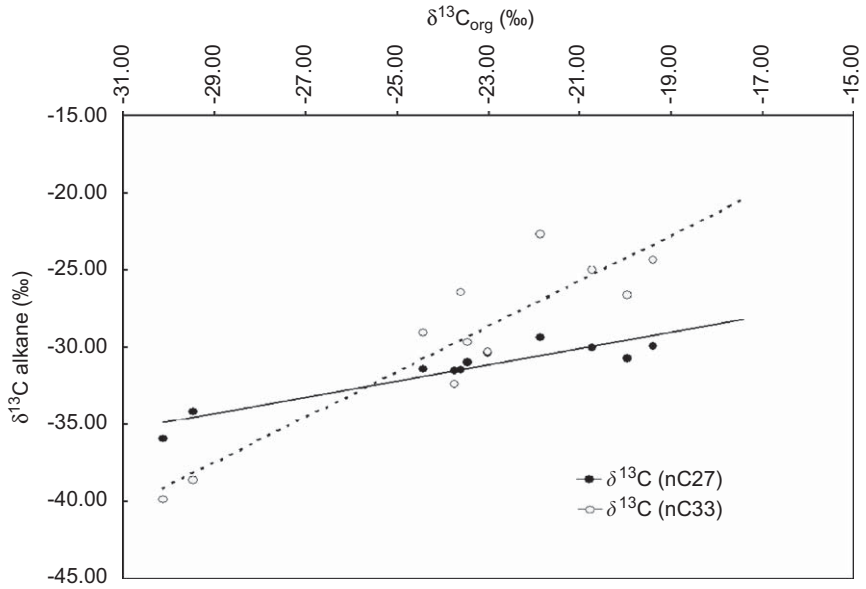

Fig. 7. Correlation between $\delta^{13}C_{org}$ and $\delta^{13}C$ of the *n*-alkanes C_{27} and C_{33} ($R > 0.91$). Modified after Zech and Glaser (2008).

OM in the record. In order to further investigate these two options, the stable carbon isotopic composition of plant-derived *n*-alkanes were analyzed.

As evident in Fig. 6b, the $\delta^{13}C$ results for the individual long-chain *n*-alkanes confirm the main $\delta^{13}C_{org}$ shifts not only in Unit C, but also in the Units A and B. The correlation coefficients for all alkanes are >0.82 ($n = 11$) (see Fig. 7 for nC_{27} and nC_{33}). This is in agreement with findings from Liu et al. (2005). Both Figs. 6b and 7 furthermore show that the amplitudes of $\delta^{13}C$ changes in the mainly grass-derived alkanes nC_{31} and nC_{33} are distinctly greater than in the alkanes nC_{27} and nC_{29}, which are additionally tree- and shrub-derived (only C3 vegetation).

These results (i) demonstrate that $\delta^{13}C$ of the alkanes nC_{31} and nC_{33} track the C3/C4 changes much more sensitively than bulk $\delta^{13}C_{org}$ and (ii) confirm that $\delta^{13}C_{org}$ is nevertheless a suitable C3/C4 proxy, whereas the plant-derived sugars do not seem to record the same palaeoenvironmental signal.

5. Synthesis: Late Quaternary palaeoenvironmental and palaeoclimatic evolution

In the following chapter we discuss the results of the multi-proxy analyses in a synthesized view and in the context with other findings in order to tentatively describe the Late Quaternary palaeoenvironmental and palaeoclimatic evolution of the study area.

5.1. Unit C: the 'Inca Huasi' wet phase (~>40 ka BP)

Unit C likely documents a period of stable environmental conditions during MIS 3 before ~40 ka BP. Note that the chronostratigraphy of the core 'Arg D4' is corroborated by other cores in the study area (a ^{14}C age of 35.7 ka cal BP was obtained for the depression Arg. 03/D2 from a buried humic-rich horizon (Table 1)). The vegetation at that time was first dominated by C3 plants with a preponderance of forests (low $\delta^{13}C_{org}$ values and low nC_{31}/nC_{27}). Possibly, even lacustrine conditions occurred in the depression (lacustrine biomarkers), indicating rather humid conditions. The end of the humid period is documented in the upper part of Unit C by a considerable increase of $\delta^{13}C_{org}$ and the alkane ratio nC_{31}/nC_{27}, indicating expansion of C4-savannah grasslands.

Comparison with other findings corroborates the interpretation of Unit C. For instance, Behling et al. (2004) and Salgado-Labouriau (1997) found palynological evidence for humid and relatively stable environmental conditions in southern Brazil during MIS 3. Evidence for a wet phase in tropical/subtropical South America between ~40 and 50 ka BP also comes from recently published speleothem records from SE Brazil (Cruz et al., 2005, 2006; Wang et al., 2006) and lake sediments from the Bolivian Altiplano (Baker et al., 2001; Fritz et al., 2004; Placzek et al., 2006) (Fig. 8). Following the argumentation of Placzek et al. (2006), their terminology is used for the respective wet phase, i.e., 'Inca Huasi', in order to avoid confusion with the formerly used term 'Minchin' (Minchin sensu Baker and Fritz corresponds to 'Inca Huasi'). From a palaeoclimatological point of view, the 'Inca Huasi' wet phase can be explained with an intensification and/or southward shift of the SASM, favored by increased austral summer insolation (Fig. 8).

5.2. C_3–C_2 hiatus: a pre-LGM dry phase (~40–20? ka BP)

In the sediment core Arg. D4, both the ^{14}C results and the elemental composition indicate a hiatus between Units C and B. Sedimentary gaps are actually quite common in tropical/subtropical South America; most pedosedimentary records

Please cite this article as: Zech, M., et al., Late Quaternary environmental changes in Misiones, subtropical NE Argentina, deduced from multi-proxy geochemical analyses in a palaeosol-sediment sequence. Quaternary International (2008), doi:10.1016/j.quaint.2008.06.006

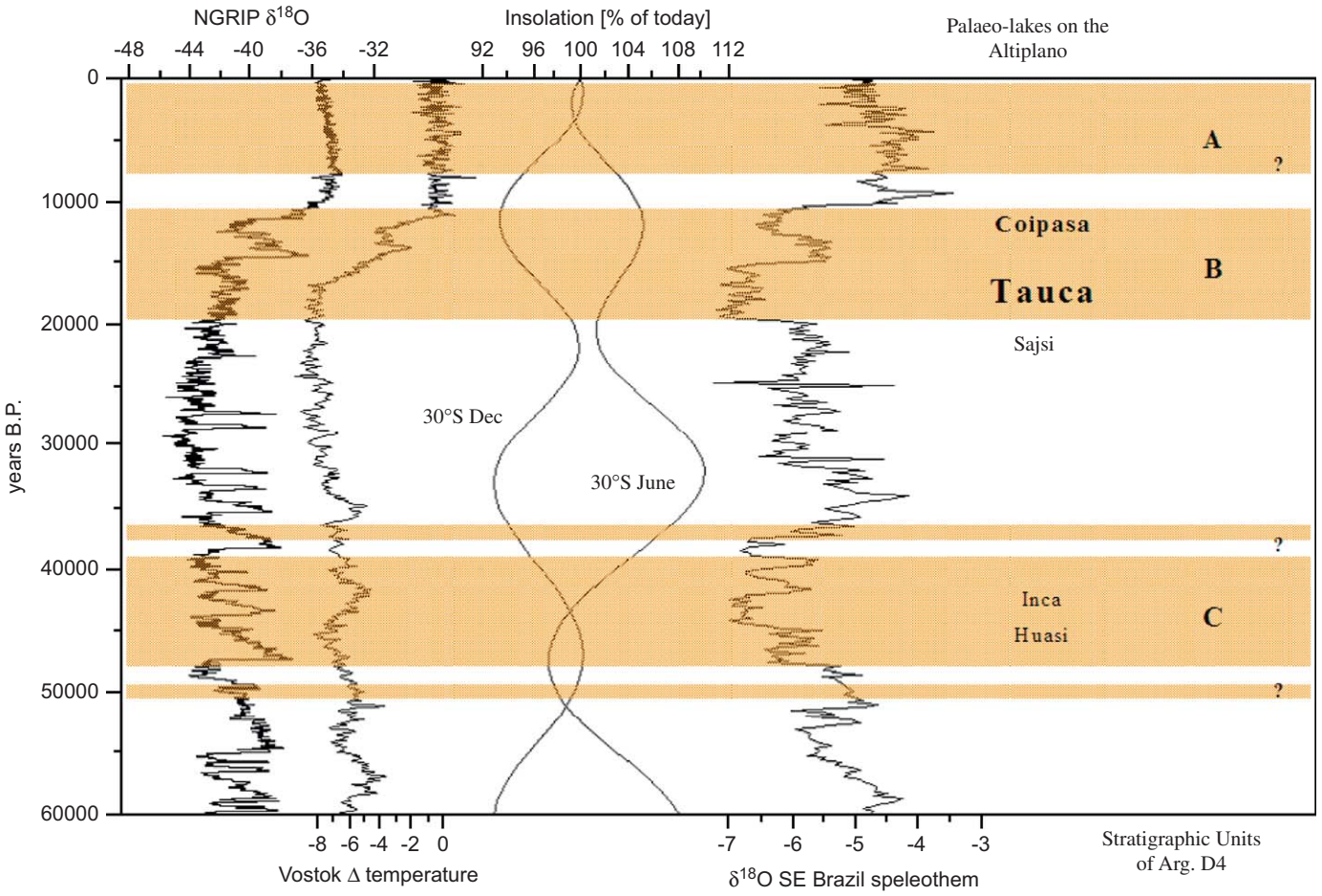

Fig. 8. Palaeoclimatic context for the sediment core Arg. D4 (periods of sedimentation are illustrated in brown shaded bars, stratigraphic units are given on the right). (a) NGRIP $\delta^{18}O$ record as temperature proxy for Greenland (NGRIP members, 2004). (b) Temperature deviation from present conditions in Antarctica derived from the Vostoc deuterium record (Petit et al., 1999). (c) Insolation changes normalized to present conditions for austral summer (30°S, December) and austral winter (30°S, June) (Berger and Loutre, 1991). (d) Speleothem $\delta^{18}O$ record from SE Brazil as proxy for the intensification of the SASM and the southward shift of the ITCZ (= more negative values) (Cruz et al., 2006). (e) Reconstructed palaeo-lakes from shoreline deposits on the Bolivian Altiplano (Placzek et al., 2006).

are discontinuous and dry conditions with intensive erosion and deflation have been inferred (e.g., Zárate, 2003; Iriondo and Kröhling, 2004; Kemp et al., 2006). Palynological findings provide evidence for the replacement of forests by savannah and grasslands due to much drier conditions in South Brazil (Behling, 2002). These changes in the vegetation cover, of course, negatively affected the overall landscape stability: Eolian activity, for example, has been documented in the southern Chaco (Iriondo, 1999) and the Paraná river basin (Stevaux, 2000), and fluvial records along the Andean Piedmont indicate the development of braided river systems with coarse gravel-beds (May et al., 2008). Very dry conditions after ~40 ka BP are also found in the speleothem records in SE Brazil and on the Altiplano (Fig. 8).

5.3. Unit B: the LGM and the subsequent Late Glacial wet phase (~20–11 ka BP)

Sedimentation and soil development in core Arg. D4 started again ~20 ka cal BP and continued during the Late Glacial (Fig. 3). This is likely corroborated by a ^{14}C age of 17.7 ka cal BP, which was obtained for a humic-rich horizon from a close-by small basin with a similar stratigraphy of the sediments (Arg. 03/P2, see Table 1). The geochemical proxies for the lower part of Unit B indicate accumulation of mainly C3-derived, relatively degraded OM during the LGM (~250–290 cm depth). During the LGM/Late Glacial transition (middle part of Unit B from ~170–250 cm depth), the SOM is still mainly C3-derived but much better preserved. Evidence for the expansion of forests during the Late Glacial (above 170 cm: ~16 ka BP) comes from the decreasing nC_{31}/nC_{27} ratios. This vegetation change presumably documents increasing precipitation, which is confirmed by other biomarker proxies, too. Also the high clay content (~70%) and the pronounced hydromorphic features in the uppermost part of Unit B (140–60 cm) indicate that again lacustrine conditions could have occurred in the small basin during the Late Glacial. The low C_{org} values, C_{org}/N ratios and HI values point to a reduced OM input and/or again more intensive SOM degradation.

Please cite this article as: Zech, M., et al., Late Quaternary environmental changes in Misiones, subtropical NE Argentina, deduced from multi-proxy geochemical analyses in a palaeosol-sediment sequence. Quaternary International (2008), doi:10.1016/j.quaint.2008.06.006

The results and the interpretation are in good agreement with other palaeoenvironmental findings. Increased precipitation during the LGM and the LGM/Late Glacial transition and hence the stabilization of the landscape due to denser vegetation can be inferred from the oxygen isotope composition in the SE Brazilian stalagmites (→intensification of the SASM) as well as from the lake sediment studies on the Altiplano. Also wet conditions during the Late Glacial are evident from the speleothem records and the lake sediments on the Altiplano ('Tauca and Coipasa' wet phase, Placzek et al., 2006; see also Fig. 8), but also from numerous other archives. Palynological and isotopic studies, for example, show Late Glacial forest expansion in NE Brazil and southern Amazon (Behling et al., 2000; Freitas et al., 2001) and cloud forests became fully developed in the Subandean Ranges of Eastern Bolivia (Mourguiart and Ledru, 2003). Besides, the transformation of the fluvial systems (from braided to meandering-river systems) indicates geomorphic stability, and consequently soil development began, e.g., along the Andean piedmont (May et al., 2008). In the Central Andes, lake transgression phases and corresponding glacial advances at that time can be traced as far south as 30°S, i.e., far beyond the present limit of the SASM (Geyh et al., 1999; Grosjean et al., 2001; Zech et al., 2006).

From a palaeoclimatic point of view, the prominent Late Glacial wet phase in tropical/subtropical South America is related to a massive intensification and southward shift of the tropical circulation (Baker et al., 2001; Cruz et al., 2005; Wang et al., 2006). Although on orbital time-scales monsoonal circulations are certainly controlled by summer insolation and resulting ocean-continental temperature and pressure gradients (e.g., Clemens et al., 1991; Gasse, 2000), the high-resolution and well-dated speleothem records clearly show that on the millennial and centennial time-scales other influencing factors must play an important role, too (Cruz et al., 2006; Wang et al., 2006). Recent modeling studies describe and emphasize the possible role of high-latitude boundary conditions, like snow and ice cover, or the thermohaline circulation (Clement et al., 2004; Chiang and Bitz, 2005; Zhang and Delworth, 2005). These models suggest that the intertropical convergence zone (ITCZ) can be rapidly shifted southward as a result of cold conditions in the northern hemisphere, as they occurred, e.g., during the Late Glacial. The southward shift of the ITCZ, which is strictly speaking a marine phenomenon, corresponds to a southward shift and an intensification of the SASM/SACZ, thus explaining increased summer precipitation over large parts of South America.

5.4. Unit A: loess deposition versus slope debris during the Holocene

The clay-rich and probably lacustrine deposits in Unit B are covered by 60 cm of almost pure silt and find sand in Unit A, which also shows a distinctly different elemental composition. This indicates changing environmental conditions since the beginning of the Holocene. The record lacks sufficient resolution to document environmental changes in the course of the Holocene, but two possible interpretations seem to be plausible:

(a) Following the suggestion of Iriondo and Kröhling (2004), Unit A could be interpreted as Holocene loess with a different sediment provenance compared to earlier eolian components contributing to the palaeosol-sediment record. Organic matter started to accumulate (increasing C_{org}) and SOM degradation is not as advanced as during the Late Glacial (increasing HI and low OI).

The palaeoclimatic interpretation in this scenario is that overall precipitation reduced due to the northward shift and weakening of the tropical circulation (Placzek et al., 2006; Cruz et al., 2006; Wang et al., 2006). Hence, new dust sources in the more arid regions west of the study area were created. At the same time, in the basin Arg. D4 probably seasonally shallow-inundated, rather swampy conditions prevailed during the Holocene period. In contrast to the proposed Late Glacial lacustrine conditions, the basin was likely stocked all the time with dust catching vegetation. The annual seasonality was reduced due to increased winter precipitation (SE trades). Intensification of the SE trades may be explained (i) by the post-glacial sea-level rise→flooding of the Argentinean shelf→proximity to the ocean and (ii) by high winter insolation→changes in the ocean-continent temperature and pressure gradient→increased moisture advection. At least for the Early Holocene, there is palaeopedological and palynological evidence for increased austral winter precipitation from the eastern Argentinean grasslands (Prieto, 2000; Mancini et al., 2005; Zech et al., 2008).

(b) The second possible interpretation of Unit A is that these upper 60 cm of this palaeosol-sediment record mainly represent slope debris coming from the catchment of the depression. One may also doubt whether Unit A has necessarily to be interpreted palaeoclimatically. On the one hand, several authors report that seasonal climate with a long annual dry period established during the Middle Holocene and fires became very frequent in tropical and subtropical South America (Freitas et al., 2001; Behling et al., 2004; Mayle et al., 2004). On the other hand, Behling et al. (2004) suggested for the close-by southern Brazil human occupation being responsible for frequent fires after 7.4 ka cal BP and Iriarte (2006) found a mid Holocene drying trend in southeastern Uruguay coinciding with major organizational changes in settlement, subsistence and technology of the pre-Hispanic populations. In both scenarios—be it climatically driven or human-induced—a destabilization of the slopes in the study area can be expected. Note that the ^{14}C ages obtained for the bottom of Unit A (Early Holocene) do

Please cite this article as: Zech, M., et al., Late Quaternary environmental changes in Misiones, subtropical NE Argentina, deduced from multi-proxy geochemical analyses in a palaeosol-sediment sequence. Quaternary International (2008), doi:10.1016/j.quaint.2008.06.006

not contradict this interpretation as they would probably overestimate the real deposition age due to the input of 'too old' SOM from the eroded soils in the catchment.

6. Conclusions

The results show that a multi-proxy approach provides much more detailed information than the standard geochemical parameters alone. The alkane ratio $n\mathrm{C}_{31}/n\mathrm{C}_{27}$, for example, turned out to be a powerful tool for reconstructing vegetation changes in terms of grass/herbs versus trees/shrubs, whereas short- and mid-chain alkanes can be used to detect lacustrine-derived OM. The validity of $\delta^{13}\mathrm{C}_{org}$ as proxy for the photosynthetic pathway of the terrestrial plants was confirmed by compound specific $\delta^{13}\mathrm{C}$ analyses on the plant-wax-derived alkanes $n\mathrm{C}_{27}$, $n\mathrm{C}_{29}$, $n\mathrm{C}_{31}$ and $n\mathrm{C}_{33}$. Accordingly, $n\mathrm{C}_{27}$—primarily derived from trees (C3)—shows smaller $\delta^{13}\mathrm{C}$ variations than the longer chain homologs, which are particularly sensitive to photosynthetic pathway changes as they mainly derive from grasses (C3 and C4). The $\delta^{13}\mathrm{C}$ values of the microbial sugars fucose and rhamnose correlate well with bulk $\delta^{13}\mathrm{C}$, likely just reflecting the food source of the microorganisms. On the contrary, $\delta^{13}\mathrm{C}$ of the plant-derived sugars arabinose and xylose exhibits a different pattern and further research will have to determine the specific compound sources to explain the observed inconsistency.

The combination of all geochemical analyses allows a tentative reconstruction of the palaeoenvironmental conditions in Misiones, i.e., in brief: stable landscape conditions, forest cover and subsequent transition to C4-grasslands (Unit C: before ~40 ka BP); landscape instability, erosive hiatus (Unit C–Unit B boundary); re-onset of sedimentation, first C3-grassland, then transition to C3-grass–tree savannah and lacustrine conditions (Unit B: LGM and Late Glacial); and, finally, Holocene sedimentation with increasing OM contribution from C4 and/or CAM-plants (Unit A).

This palaeoclimatic interpretation is in good agreement with fluvial, palynological, speleothem and lacustrine data from tropical/subtropical South America and suggests that variations in the intensity and/or latitudinal shifts of the tropical circulation (SASM and SACZ) play an important role for the palaeoenvironmental conditions: The sediment core Arg. D4 likely records (i) the 'Inca Huasi' wet phase (~>40 ka BP), (ii) a dry phase of pronounced landscape instability and erosion during the pre-LGM, (iii) the transition from intermediate environmental conditions during the LGM to the pronounced Late Glacial wet phase, which probably documents the phase of the most intensive and southward shifted tropical circulation, and (iv) finally, the establishment of the Holocene atmospheric circulation pattern.

Ongoing research now focuses on palynological work in order to confirm the reconstructed vegetation history. Besides, further analytical developments, like $\delta^{18}\mathrm{O}$ and deuterium analyses in OM and especially in specific compounds, are being tested to obtain additional palaeoclimatic information from terrestrial sediments.

Acknowledgements

We would like to thank J. Eidam from University of Greifswald for X-ray fluorescence analysis and B.M. Krooß from the RWTH Aachen for outlining the Rock-Eval pyrolysis. We are also very grateful to T. Gonter, M. Haider, I. Thaufelder and L. Sauheitl for assistance during laboratory work.

References

Amelung, W., Cheshire, M.V., Guggenberger, G., 1996. Determination of neutral and acidic sugars in soil by capillary gas–liquid chromatography after trifluoroacetic acid hydrolysis. Soil Biology and Biochemistry 28, 1631–1639.

Ariztegui, D., Chondrogianni, C., Lami, A., Giulizzoni, P., Lafargue, E., 2001. Lacustrine organic matter and the Holocene paleoenvironmental record of Lake Albano (central Italy). Journal of Paleolimnology 26, 283–292.

Aucour, A.-M., Hillaire-Marcel, C., Bonnefille, R., 1999. Sources and accumulation rates of organic carbon in an equatorial peat bog (Burundi, East Africa) during the Holocene: carbon isotope constraints. Palaeogeography, Palaeoclimatology, Palaeoecology 150, 179–189.

Baker, P.A., Rigsby, C.A., Seltzer, G.O., Fritz, S.C., Lowenstein, T.K., Bacher, N.P., Veliz, C., 2001. Tropical climate changes at millennial and orbital timescales on the Bolivian Altiplano. Nature 409, 698–701.

Behling, H., 2002. South and southeast Brazilian grasslands during Late Quaternary times: a synthesis. Palaeogeography, Palaeoclimatology, Palaeoecology 177, 19–27.

Behling, H., Arz, H.W., Pätzold, J., Wefer, G., 2000. Late Quaternary vegetational and climate dynamics in northeastern Brazil, inferences from marine core GeoB 3104-1. Quaternary Science Reviews 19, 981–994.

Behling, H., Pillar, V., Orlóci, L., Bauermann, S.G., 2004. Late Quaternary Araucaria forest, grassland (Campos), fire and climate dynamics, studied by high-resolution pollen, charcoal and multivariate analysis of the Cambará do Sul core in southern Brazil. Palaeogeography, Palaeoclimatology, Palaeoecology 203, 277–297.

Berger, A.L., Loutre, M.F., 1991. Insolation values for the climate of the last 10 million years. Quaternary Science Reviews 10 (4), 297–317.

Bourbonniere, R.A., Telford, S.L., Ziolkowski, L.A., Lee, J., Evans, M.S., Meyers, P.A., 1997. Biogeochemical marker profiles in cores of dated sediments from large North American lakes. In: Eganhouse, R.P. (Ed.), Molecular Markers in Environmental Geochemistry, ACS Symposium Series. American Chemical Society, Washington, DC, pp. 133–150.

Cerveny, R.S., 1998. Present climates of South America. In: B.H.A. (Ed.), Climates of the Southern Continents: Present, Past and Future. Wiley.

Chiang, J., Bitz, C., 2005. Influence of high latitude ice cover on the marine Intertropical Convergence Zone. Climate Dynamics 25 (5), 477–496.

Clemens, S.C., Prell, W.L., Murray, D., Shimmield, G., Weedon, G., 1991. Forcing mechanisms of the Indian Ocean monsoon. Nature 353, 720–725.

Clement, A.C., Hall, A., Broccoli, A.J., 2004. The importance of precessional signals in the tropical climate. Climate Dynamics 22 (4), 327–341.

Collatz, G.J., Berry, J.A., Clark, J.S., 1998. Effects of climate and atmospheric CO_2 partial pressure on global distribution of C4 grasses: present, past and future. Oecologia 114, 441–454.

Please cite this article as: Zech, M., et al., Late Quaternary environmental changes in Misiones, subtropical NE Argentina, deduced from multi-proxy geochemical analyses in a palaeosol-sediment sequence. Quaternary International (2008), doi:10.1016/j.quaint.2008.06.006

Collister, J.W., Rieley, G., Stern, B., Eglington, G., Fry, B., 1994. Compound-specific $\delta^{13}C$ analyses of leaf lipids from plants with differing carbon dioxide metabolism. Organic Geochemistry 21, 619–627.

Cranwell, P.A., 1973. Chain-length distribution of *n*-alkanes from lake sediments in relation to post-glacial environmental change. Freshwater Biology 3, 259–265.

Cranwell, P.A., 1981. Diagenesis of free and bound lipids in terrestrial detritus deposited in lacustrine sediments. Organic Geochemistry 3, 79–89.

Cruz, F.W., Burns, S.J., Karmann, I., Sharp, W.D., Vuille, M., Cardoso, A.O., Ferrari, J.A., Dias, P.L., Viana, O., 2005. Insolation-driven changes in atmospheric circulation over the past 116,000 years in subtropical Brazil. Nature 434, 63–65.

Cruz, F.W., Burns, S.J., Karmann, I., Sharp, W.D., Vuille, M., 2006. Reconstruction of regional atmospheric circulation features during the Late Pleistocene in subtropical Brazil from oxygen isotope composition of speleothems. Earth and Planetary Science Letters 248 (1), 495–507.

Disnar, J.R., Guillet, B., Keravis, D., Di-Giovanni, C., Sebag, D., 2003. Soil organic matter (SOM) characterization by Rock-Eval pyrolysis: scope and limitations. Organic Geochemistry 34, 327–343.

Espitalie, J., Deroo, J., Marquis, F., 1985. Rock-Eval pyrolysis and its applications. Institut Francais du Pétrole, Report #33578.

Farrimond, P., Flanagan, R.L., 1996. Lipid stratigraphy of a Flandrian peat bed (Northumberland, UK): comparison with the pollen record. The Holocene 6 (1), 67–74.

Feng, X., 2002. A theoretical analysis of carbon isotope evolution of decomposing plant litters and soil organic matter. Global Biogeochemical Cycles 16, 1–10.

Fernández, R.A., Lupi, A.M., Parh, N., 1999. Aptitud de las tierras para la implantación de bosques. Provincia de Misiones. Yvyraretá, 9.

Ficken, K.J., Barber, K.E., Eglinton, G., 1998. Lipid biomarker, $d^{13}C$ and plant macrofossil stratigraphy of a Scottish montane peat bog over the last two millennia. Organic Geochemistry 28 (3/4), 217–237.

Ficken, K.J., Li, B., Swain, D.L., Eglinton, G., 2000. An *n*-alkane proxy for the sedimentary input of submerged/floating freshwater aquatic macrophytes. Organic Geochemistry 31, 745–749.

Filippi, M.L., Talbot, M.R., 2005. The palaeolimnology of northern Lake Malawi over the last 25 ka based upon the elemental and stable isotopic composition of sedimentary organic matter. Quatenary Science Reviews 24, 1303–1328.

Freitas, H.A., Pessenda, L.C., Aravena, R., Gouveia, S.E., Ribeiro, A.S., Boulet, R., 2001. Late Quaternary vegetation dynamics in the Southern Amazon Basin inferred from carbon isotopes in soil organic matter. Quaternary Research 55, 39–46.

Fritz, S.C., Baker, P.A., Lowenstein, T.K., Seltzer, G.O., Rigsby, C.A., Dwyer, G.S., Tapia, P.M., Kimberly, K.A., Ku, T.-L., Luo, S., 2004. Hydrologic variation during the last 170,000 years in the southern hemisphere tropics of South America. Quaternary Research 61, 95–104.

Gallet, S., Jahn, B., Van Vliet Lanoe, B., Dia, A., Rossello, E., 1998. Loess geochemistry and its implications for particle origin and composition of the upper continental crust. Earth and Planetary Science Letters 156, 157–172.

Gan, M.A., Kousky, V.E., Ropelewski, C.F., 2004. The South American monsoon circulation and its relationship to rainfall over West-Central Brazil. Journal of Climate 17, 47–66.

Garrels, R.M., Mackenzie, F.T., 1971. Evolution of Sedimentary Rocks. Norton, New York, p. 397.

Gasse, F., 2000. Hydrological changes in the African tropics since the Last Glacial Maximum. Quaternary Science Reviews 19, 189–211.

Geyh, M.A., Schleicher, H., 1991. Absolute Age Determination. Springer, New York.

Geyh, M.A., Grosjean, M., Nunez, L., Schotterer, U., 1999. Radiocarbon reservoir effect and the timing of the Late-Glacial/Early Holocene humid phase in the Atacama Desert (Northern Chile). Quaternary Research 52, 143–153.

Glaser, B., 2005. Compound-specific stable-isotope ($\delta^{13}C$) analysis in soil science. Journal of Plant Nutrition and Soil Science 168, 633–648.

Glaser, B., Amelung, W., 2002. Determination of ^{13}C natural abundance of amino acid enantiomers in soil: methodological considerations and first results. Rapid Communications in Mass Spectrometry 16, 891–898.

Glaser, B., Zech, W., 2005. Reconstruction of climate and landscape changes in a high mountain lake catchment in the Gorkha Himal, Nepal during the Late Glacial and Holocene as deduced from radiocarbon and compound-specific stable isotope analysis of terrestrial, aquatic and microbial biomarkers. Organic Geochemistry 36, 1086–1098.

Grosjean, M., van Leeuwen, J.F.N., van der Knaap, W.O., Geyh, M.A., Ammann, B., Tanner, W., Messerli, B., Veit, H., 2001. A 22,000 ^{14}C yr BP sediment and pollen record of climate change from Laguna Miscanti 231S, northern Chile. Global and Planetary Change 28, 35–51.

Gross, S., Glaser, B., 2004. Minimization of foreign carbon addition during derivatization of organic molecules for compound-specific $\delta^{13}C$ analysis of soil organic matter. Rapid Communications in Mass Spectrometry 18, 2753–2764.

Huang, Y., Bol, R., Harkness, D.D., Ineson, P., Eglington, G., 1996. Post-glacial variations in distributions, ^{13}C and ^{14}C contents of aliphatic hydrocarbons and bulk organic matter in three types of British acid upland soils. Organic Geochemistry 24 (3), 273–287.

Huang, Y., Street-Perrott, F.A., Metcalfe, S.A., Brenner, M., Moreland, M., Freeman, K.H., 2001. Climate change as the dominant control on glacial–interglacial variations in C_3 and C_4 plant abundance. Science 293, 1647–1651.

Hueck, K., Seibert, P., 1972. Vegetationskarte von Südamerika. Vegetationsmonographien der einzelnen Großräume, Band II a. Gustav Fischer Verlag, Stuttgart.

Iriarte, J., 2006. Vegetation and climate change since 14,810 ^{14}C yr BP in southeastern Uruguay and implications for the rise of early formative societies. Quaternary Research 65, 20–32.

Iriondo, M., 1999. Climatic changes in the South American plains: Records of a continent-scale oscillation. Quaternary International 57/58, 93–112.

Iriondo, M., Kröhling, D.M., 2004. The parent material as the dominant factor in Holocene pedogenesis in the Uruguay River Basin. Revista Mexicana de Ciencias Geológicas 21 (1), 175–184.

Kemp, R.A., Zárate, M.A., Toms, P., King, M., Sanabria, J. and Arguello, G., 2006. Late Quaternary paleosols, stratigraphy and landscape evolution in the Northern Pampa, Argentina. Quaternary Research.

Kolattukudy, P.E., 1976. Biochemistry of plant waxes. In: Kolattukudy (Ed.), Chemistry and Biochemistry of Natural Waxes. Elsevier, Amsterdam, pp. 290–349.

Kröhling, D.M., Iriondo, M., 1999. Upper Quaternary palaeoclimates of the Mar Chiquita area, North Pampa, Argentina. Quaternary International 57/58, 149–163.

Kronberg, B.I., Nesbitt, H.W., 1981. Quantification of weathering soil chemistry and soil fertility. Journal of Soil Science 32, 453–459.

Lichtfouse, E., 1998. Isotope and biosynthetic evidence for the origin of long-chain aliphatic lipids in soils. Naturwissenschaften 85, 76–77.

Ligier, H., Mattelo, H., Polo, H., Rosso, J., 1990. Provincia de Misiones, escala 1:500.000. Atlas de Suelos de la República Argentina. SAGyP-INTA, pp. 109–154.

Liu, W., Huang, Y., An, Z., Clemens, S.C., Li, L., Prell, W.L., Ning, Y., 2005. Summer monsoon intensity controls C4/C3 plant abundance during the last 35 ka in the Chinese loess plateau: carbon isotope evidence from bulk organic matter and individual leaf waxes. Palaeogeography, Palaeoclimatology, Palaeoecology 220, 243–254.

Lüniger, G., Schwark, L., 2002. Characterisation of sedimentary organic matter by bulk and molecular geochemical proxies: an example from Oligocene maar-type Lake Enspel, Germany. Sedimentary Geology 148, 275–288.

Please cite this article as: Zech, M., et al., Late Quaternary environmental changes in Misiones, subtropical NE Argentina, deduced from multi-proxy geochemical analyses in a palaeosol-sediment sequence. Quaternary International (2008), doi:10.1016/j.quaint.2008.06.006

Mancini, M.V., Paez, M.M., Prieto, A.R., Stutz, S., Tonello, M., Vilanova, I., 2005. Mid-Holocene climatic variability reconstruction from pollen records (32°–52°S, Argentina). Quaternary International 132, 47–59.

Margalot, J.A., 1985. Geografía de Misiones. Industria Gráfica del Libro, Buenos Aires, p. 236.

May, J.-H., Zech, R., Veit, H., 2008. Late Quaternary paleosol-sediment-sequences and landscape evolution along the Andean piedmont, Bolivian Chaco. Geomorphology 98 (1), 34–54.

Mayle, F.E., Beerling, D.J., Gosling, W.D., Bush, M.B., 2004. Responses of Amazonian ecosystems to climatic and atmospheric carbon dioxide changes since the Last Glacial Maximum. doi:10.1098/rstb.2003.1434.

McLennan, S.M., 1993. Weathering and global denudation. Journal of Geology 101, 295–303.

Meyers, P.A., Ishiwatari, R., 1993. Lacustrine organic matter geochemistry—an overview of indicators of organic matter sources and diagenesis in lake sediments. Organic Geochemistry 20 (7), 867–900.

Morrás, H., Moretti, L., Píccolo, G., Zech, W., 2005. New hypotheses and results about the origin of stonelines and subsurface structured horizons in ferrallitic soils of Misiones, Argentina. Geophysical Research Abstracts 7, 05522.

Morrás, H., Moretti, L., Piccolo, G., Zech, W., 2008. About the genesis of subtropical soils with stony horizons in NE Argentina: Authochtony and polygenesis—a review. Quartenary International, this issue.

Mourguiart, P., Ledru, M.-P., 2003. Last Glacial maximum in an Andean cloud forest environment (Eastern Cordillera, Bolivia). Geology 31 (3), 195–198.

Muhs, D.R., Ager, T.A., Bettis III, E.A., McGeehin, J., Been, J.M., Begét, J.E., Pavich, M.J., Stafford Jr., T.W., Stevens, S.P., 2004. Stratigraphy and palaeoclimatic significance of Late Quaternary loess–palaeosol sequences of the Last Interglacial–Glacial cycle in central Alaska. Quaternary Science Reviews 22, 1947–1986.

Muhs et al., this issue.

NGRIP members, 2004. High-resolution record of Northern Hemisphere climate extending into the last interglacial period. Nature 431, 147–151.

Nott, C.J., Xie, S., Avsejs, L.A., Maddy, D., Chambers, F.M., Evershed, R.P., 2000. *n*-Alkane distributions in ombrotrophic mires as indicators of vegetation change related to climatic variation. Organic Geochemistry 31, 231–235.

Petit, J.R., Jouzel, J., Raynaud, D., Barkov, N.I., Barnola, J.-M., Basile, I., Bender, M., Chappellaz, J., Davis, M., Delaygue, G., Delmotte, M., Kotlyakov, V.M., Legrand, M., Lipenkov, V.Y., Lorius, C., Pépin, L., Ritz, C., Saltzman, E., Stievenard, M., 1999. Climate and atmospheric history of the past 420,000 years from the Vostoc ice core, Antarctica. Nature 399, 429–436.

Placzek, C., Quade, J., Patchett, P.J., 2006. Geochronology and stratigraphy of Late Pleistocene lake cycles on the southern Bolivian Altiplano: implications for causes of tropical climate change. Geological Society of America Bulletin 118 (5–6), 515–532.

Prieto, A.R., 2000. Vegetational history of the Late glacial–Holocene transition in the grasslands of eastern Argentina. Palaeogeography, Palaeoclimatology, Palaeoecology 157, 167–188.

Prohaska, F., 1976. The Climate of Argentina, Paraquay and Uruquay. In: Schwertfeger, W. (Ed.), Climates of Central and South America. Elsevier Scientific Publishing Company, Amsterdam.

quickcal2005 version 1.4, 〈http://www.calpal-online.de〉.—Copyright 2003–2005, CalPal Authors.

Salgado-Labouriau, M.L., 1997. Late Quaternary palaeoclimate in the savannas of South America. Journal of Quaternary Science 12 (5), 371–379.

Schmitt, J., Glaser, B., Zech, W., 2003. Amount-dependent isotopic fractionation during compound-specific isotope analysis. Rapid Communications in Mass Spectrometry 17, 970–977.

Schwark, L., Zink, K., Lechtenbeck, J., 2002. Reconstruction of postglacial to early Holocene vegetation history in terrestrial Central Europe via cuticular lipid biomarkers and pollen records from lake sediments. Geology 30 (5), 463–466.

Silliman, J.E., Meyers, P.A., Bourbonniere, R.A., 1996. Record of postglacial organic matter delivery and burial in sediments of Lake Ontario. Organic Geochemistry 24, 463–472.

Stevaux, J.C., 2000. Climatic events during the Late Pleistocene and Holocene in the Upper Parana River: correlation with NE Argentina and South-Central Brazil. Quaternary International 72, 73–85.

Street-Perrott, F.A., Huang, Y., Perrott, R.A., Eglinton, G., Barker, P., Khelifa, L., Harkness, D.D., Olago, D.O., 1997. Impact of lower atmospheric CO_2 on tropical mountain ecosystems. Science 278, 1422–1426.

Street-Perrott, F.A., Ficken, K.J., Huang, Y., Eglington, G., 2004. Late Quaternary changes in carbon cycling on Mt. Kenya, East Africa: an overview of the $\delta^{13}C$ record in lacustrine organic matter. Quaternary Science Reviews 23, 861–879.

Teruggi, M.E., 1957. The nature and origin of Argentine loess. Journal of Sedimentary Petrology 27, 322–332.

Thompson, L.G., Davis, M.E., Mosley-Thompson, E., Lin, P.-N., Henderson, K.A., Mashiotta, T.A., 2005. Tropical ice core records: evidence for asynchronous glaciation on Milankovitch timescales. Journal of Quaternary Science 20 (7–8), 723–733.

van Dongen, B.E., Schouten, S., Sinninghe Damasté, J.S., 2002. Carbon isotope variability in monosaccharides and lipids of aquatic algae and terrestrial plants. Marine Ecology Progress Series 232, 83–92.

Vera, C.S., Vigliarolo, P.K., Berbery, E.H., 2002. Cold season synoptic-scale waves over subtropical South America. Monthly Weather Review 130, 684–699.

Wang, H., Follmer, L.R., Liu, C.-L.J., 2000. Isotope evidence of paleo-El Niño-Southern Oscillation cycles in loess–paleosol record in the central United States. Geology 28 (9), 771–774.

Wang, X., Auler, A.S., Edwards, R.L., Cheng, H., Ito, E., Solheid, M., 2006. Interhemispheric anti-phasing of rainfall during the last glacial period. Quaternary Science Reviews 25 (23–24), 3391–3403.

Zárate, M.A., 2003. Loess of southern South America. Quaternary Science Reviews 22, 1987–2006.

Zech, M., 2006. Evidence for Late Pleistocene climate changes from buried soils on the southern slopes of Mt. Kilimanjaro, Tanzania. Palaeogeography, Palaeoclimatology, Palaeoecology 242, 303–312.

Zech, M., Glaser, B., 2008. Improved compound-specific $\delta^{13}C$ analysis of *n*-alkanes for application in palaeoenvironmental studies. Rapid Communications in Mass Spectrometry 22, 135–142.

Zech, R., Kull, C., Veit, H., 2006. Late Quaternary glacial history in the Encierro Valley, northern Chile (29°S), deduced from ^{10}Be surface exposure dating. Palaeogeography, Palaeoclimatology, Palaeoecology 234, 277–286.

Zech, M., Zech, R., Glaser, B., 2007. A 240,000-year stable carbon and nitrogen isotope record from a loess-like palaeosol sequence in the Tumara Valley, Northeast Siberia. Chemical Geology 242, 307–318.

Zech, W., Zech, M., Zech, R., Peinemann, N., Morrás, H.J.M., Moretti, L., Ogle, N., Kalim, R.M., Fuchs, M., Schad, P., Glaser, B., 2008. Late Quaternary palaeosol records from subtropical (38°S) to tropical (16°S) South America and palaeoclimatic implications. Quaternary International, this issue.

Zeil, W., 1986. Südamerika. Geologie der Erde Band 1. Ferdinand Enke Verlag, Stuttgart.

Zhang, R., Delworth, T.L., 2005. Simulated tropical response to a substantial weakening of the Atlantic Thermohaline circulation. Journal of Climate 18 (12), 1853–1860.

Zhang, Z., Zhao, M., Yang, X., Wang, S., Jiang, X., Oldfield, F., Eglinton, G., 2004. A hydrocarbon biomarker record for the last 40 kyr of plant input to Lake Heqing, southwestern China. Organic Geochemistry 35, 595–613.

Zhou, J.Y., Lau, K.-M., 1998. Does a monsoon climate exist over South America? Journal of Climate 11, 1020–1040.

Please cite this article as: Zech, M., et al., Late Quaternary environmental changes in Misiones, subtropical NE Argentina, deduced from multi-proxy geochemical analyses in a palaeosol-sediment sequence. Quaternary International (2008), doi:10.1016/j.quaint.2008.06.006